



Algal Biochar: Enhancing Phyto-Bioremediation for Heavy Metals Removal

Ashgan A. Abou Gabal¹, Nader Saad Elsayed^{2, 3}, Hesham M. Aly⁴, Hoda F. Zahran⁵,
Asmaa A. Khaled⁶, Haiam M. Aboul-Ela⁷, Ola Kh. Shalaby^{8*}

¹Agricultural Botany Department, Faculty of Agriculture, Saba Basha, Alexandria University, Egypt

²College of Resources, Hunan Agricultural University, Changsha, China

³Soil and Agricultural Chemistry Department, Faculty of Agriculture (Saba-Basha), Alexandria University, Alexandria, Egypt

⁴Horticulture Institute, Department of Forestry and Wood Technology, Antoniadis Botanical Garden, Agriculture Research Center, Alexandria, Egypt

⁵Pollution Management Department, Environment and Natural Materials Research Institute, City of Scientific Research and Technological Applications (SRTA-City), New Borg Al-Arab City 21934, Alexandria, Egypt

⁶Animal and Fish Production Department, Faculty of Agriculture, Alexandria University, Egypt

⁷College of Fisheries and Aquaculture Technology, Arab Academy for Science, Technology, and Maritime Transport, Alexandria, Egypt

⁸National Institute of Oceanography and Fisheries (NIOF), Egypt

*Corresponding Author: ola_shalaby2012@yahoo.com

ARTICLE INFO

Article History:

Received: Oct. 25, 2024

Accepted: Dec. 1st, 2024

Online: Dec. 4, 2024

Keywords:

Marine macroalgae,
Bioaccumulation,
Pyrolysis,
Sustainable remediation,
Environmental monitoring

ABSTRACT

Heavy metals (HMs) contamination in the Eastern Harbor (EH), Alexandria, Egypt, presents serious environmental and health concerns. Increased industrial activities and urban runoff have raised pollutant levels in the area, impacting marine ecosystems and water quality. This study investigated the potential of biochar (BC) derived from marine macroalgae for removing (HM) ions from contaminated aqueous solutions. Biochar was produced through pyrolysis at 500°C, and its adsorption capacity was evaluated for the removal of Pb, Cu, Ni, Zn, and Cd. The physicochemical analysis revealed that marine macroalgae-derived biochar demonstrated exceptional removal efficiencies, ranging from 97 to 99% for the targeted (HMs). Among the macroalgae species assessed, *Corallina officinalis* was the most efficient bioaccumulator of Pb, Ni, and Cd, while *Ulva compressa* and *Ulva fasciata* showed the highest bioaccumulation of Fe, Cu, and Mn. These results highlighted the significant potential of algal biochar as a sustainable and effective material for the removal of HMs from contaminated water, offering an eco-friendly solution for pollution control and contributing to the development of circular economy practices.

INTRODUCTION

HMs (Heavy Metals) are characterized by a specific density greater than 5g/ cm³, which is a primary cause of precipitation and accumulation in aquatic ecosystems (Rasheed *et al.*, 2024). They are non-biodegradable and bioaccumulating substances, known to be toxic to living organisms, even at very low concentrations (Fu & Wang,

2011). Therefore, the removal of HMs is essential. Various remediation techniques, based on either mobilization or immobilization processes, have been developed to address these challenges (Ahmed *et al.*, 2022; Salaah *et al.*, 2022).

Algal diversity plays a crucial ecological role in coastal ecosystems by cycling carbon, nitrogen, and phosphorus. It helps regulate water quality, provides habitat, supports coastal food webs, and contributes to overall productivity and biodiversity (Abou Gabal *et al.*, 2022). Algae can accumulate trace metals, reaching concentration values that are thousands of times higher than their corresponding concentration in seawater (Conti & Cecchetti, 2003). The use of macroalgae in biomonitoring indicates that metal concentrations in macroalgae correspond to bioavailable metal concentrations in marine ecosystems (Campanella *et al.*, 2001). Marine macroalgae are widely used in coastal waters around the world as bioindicators of metal contamination (Okuku & Peter, 2012). A key assumption in using seaweeds as bioindicators is that the metal concentrations in the algae are directly proportional to the bioavailable metal concentrations in the surrounding environment. Macroalgae are particularly effective in studies of heavy metal pollution due to their rapid accumulation of metals from water and their ability to concentrate dissolved metals in their cell walls (Salgado *et al.*, 2005).

Based on environmentally friendly and financially viable aspects, considerable attention has been devoted to the application of biochar (BC) as a practical approach because of its low cost, the wide range of available feedstock materials, as well as mechanical and thermal stability (Mohan *et al.*, 2015). BC is recognized as a versatile material for addressing HMs in contaminated soils and water (Lehmann *et al.*, 2011).

BC is typically produced through the thermal treatment of biomass, such as wood, manure, or leaves, in an oxygen-free environment. It has gained significant attention due to its unique physio-chemical properties and its wide range of applications across various fields, including climate change mitigation, agriculture, environmental remediation, and energy production (Premarathna *et al.*, 2019).

BC is a sustainable, carbon-neutral material, with CO₂ emissions during its production balanced by the amount absorbed by the biomass during photosynthesis (Yuan *et al.*, 2019). Its porous structure makes it an effective carbon storage solution and aids in pollutant adsorption and degradation. BC is made from various carbon-rich feedstocks, often organic waste, supporting waste management efforts. Due to its cost-effectiveness, BC is used in water and soil treatment as an affordable alternative to activated carbon for removing contaminants like heavy metals, pesticides, and dyes (Zhao *et al.*, 2021). However, its low surface area limits its effectiveness, prompting research into enhancing its properties through modification techniques such as amination, acid/base treatments, and magnetic modification (Arif *et al.*, 2021).

BC can significantly adsorb HMs, resulting in decreased bio-availability and leaching of these metals (Cui *et al.*, 2019). With recent advancements in BC research, different raw materials have been utilized to successfully eliminate HMs, sawdust

(Kaczala *et al.*, 2009), dairy manure (Kolodyńska *et al.*, 2012), wastewater sludge (Zhang *et al.*, 2013), organic waste (Mohan *et al.*, 2014), terrestrial biomass, such as wood, agricultural residues, and peanut shells (Zhang *et al.*, 2015) in addition to energy cane (Mohan *et al.*, 2015). More recently, biochar derived from microalgae and marine macroalgae have attracted more attention in research because they are easy to grow and has high production rates (González-Hourcade *et al.*, 2022; Kenneth *et al.*, 2023).

The main goal of this research was to identify the most prevalent algae species at each selected site concerning their accumulation of common HMs, specifically cadmium, zinc, copper, lead, and iron. Additionally, the research aimed to identify macroalgae species with the highest metal retention capabilities for targeted use in phytoremediation of contaminated sites. Furthermore, the research investigated the characteristics of BC derived from the specified marine macroalgae and assessed its ability to eliminate HMs from water solutions, thus aiding in bioremediation endeavors.

MATERIALS AND METHODS

1. Study area

The Eastern Harbor (EH) is a shallow semi-closed basin covering an area of around 2.8km², situated in the central portion of Alexandria, Egypt, with an average depth of 6.5m and a water volume of 16.44 ×10⁶ m³. Concrete blocks also fortified the southern portion of the harbor; the northern side is protected by an artificial breakwater with eastern and western inlets. It is bordered to the east by a land projection, El-Silsila, and to the northwest by a long causeway. In addition to shipping operations and agriculture, the receipt of sewage effluents from many small sewers as a Hunting Club and Yacht Club, the Eastern Harbor is impaired by the sewage drainage of the central section of Alexandria City, also, to waste from fishing and sailing boats anchoring within the harbor around 5400m of sewage per hour. The port is separated by an artificial breakwater of concrete blocks from the open sea, except for two openings on the middle and eastern sides of the breakwater that allow the active exchange of water between the port and the open sea (Abou Gabal *et al.*, 2023; Khairy *et al.*, 2024).

1.1. Location

Eastern Harbor (EH) is located at latitude 31°12'02.5" and longitude 29°53'33.4" (Fig. 1).



Fig. 1. Sampling area (Eastern Harbor), Alexandria, Egypt

2. Sampling procedures

Seawater samples were collected in June 2019 from a depth of 0.5 meters in the Eastern Harbor (EH) using acid-washed polyethylene bottles. Macroalgae samples were handpicked at low tide from intertidal zones, ensuring minimal disturbance to the habitat. Each sample was thoroughly rinsed with deionized water to remove debris and epiphytes before further processing.

2.1. Macroalgae identification

According to taxonomic studies by **Khalil (1987)** and **Aleem (1993)**, the Eastern Harbor was found to host three species: *Ulva fasciata*, *Ulva compressa*, and *Corallina officinalis* (**El-Din *et al.*, 2015**; **AbouGabal *et al.*, 2021**; **Ibrahim *et al.*, 2024**).

2.2. Sample preparation and analysis of HMs in seawater and macroalgae

Seawater analysis:

- **Collection:** Seawater samples were collected from the Eastern Harbor (EH) in June 2019 at 0.5 meters depth using acid-washed polyethylene bottles.
- **Preservation and extraction:** Samples were acidified with nitric acid and metals were extracted using APDC and MIBK solvents.
- **Analysis:** Metal concentrations were measured by atomic absorption spectrophotometry (AAS) following **APHA (2017)** standards.

Macroalgae analysis:

- **Preparation:** Algae (*Ulva fasciata*, *Ulva compressa*, *Corallina officinalis*) were washed, dried at 40°C, and grounded into powder.

- **Digestion:** Algae samples were digested with nitric and hydrochloric acids, filtered, and diluted.
- **Analysis:** Metal concentrations were measured using atomic absorption spectrophotometry (AAS), following **AOAC (1990)** protocols.

Blank controls and replicates:

Blank controls (deionized water) were used to ensure accuracy. All analyses were performed in triplicate for reliability.

2.3. Preparation and pyrolysis of algae

The algae were initially washed with deionized water to remove impurities, and then air-dried before undergoing pyrolysis.

2.3.1. Pyrolysis process

The thermo chemical conversion of seawater algae into BC was performed in an electrically heated muffle furnace (*Model. HD-150*, Spain). Close to 15gm of algae samples were weighed and put in crucibles with secure lids. The pyrolysis was carried out under oxygen-limited conditions without nitrogen gas flow. The heat was gradually increased to 500°C at a rate of about 15°C per minute, and held at that temperature for one hour. This temperature was chosen based on literature indicating it as optimal for BC production and maximum heavy metal adsorption efficiency (**Vargas & Monteggia 2015**). Following pyrolysis, the BC was cooled to room temperature, subsequently grounded, and then stored in sealed bags until further use.

2.4. Surface morphology and characterization

2.4.1. Scanning electron microscopy (SEM) analysis

SEM was used to investigate the surface of each of the three algal BC samples and to examine their morphology, which was observed after gold coating on a copper holder, using a JSM 6360LA from JEOL, Japan, at an accelerating voltage of 20 KV.

By applying Fourier transform infrared (FTIR) analysis, the composition of three algal biochar samples and their surface functional groups were obtained using Fourier transform infrared (Bruker ALFA FTIR spectrometer—Bruker Corporation, Ettlingen, Germany) in a range between 400 and 3900cm⁻¹.

2.4.2. The thermo gravimetric analyzer (TGA)

The thermal stability of the three algal biochar samples was assessed using a thermogravimetric analyzer (TGA-50 Shimadzu).

2.4.3. Particle size analyzer (PSA)

Particle size distribution for the three algal BC samples was analyzed using a submicron particle size analyzer (Beckman Coulter—USA). The samples were dispersed in water at a temperature of 20°C, with a viscosity of 1.002 and a refractive index of 1.33.

2.5. Biosorption studies

2.5.1. Preparation of metal solutions

Metal salts ($\text{CdCl}_2 \cdot \text{H}_2\text{O}$, $\text{Pb}(\text{NO}_3)_2$, $\text{CuSO}_4 \cdot 5\text{H}_2\text{O}$, $\text{NiCl}_2 \cdot 6\text{H}_2\text{O}$, and $\text{ZnSO}_4 \cdot 7\text{H}_2\text{O}$) were dissolved in deionized water to prepare 50mg/ L stock solutions. To evaluate the impact of initial metal concentration on adsorption, various metals (Zn, Cu, Cd, Ni, and Pb) were tested.

2.5.2. Batch adsorption experiments

- 0.5g of BC was added to 100mL conical flasks containing 50mL of each 50mg/ L metal solution.
- All experiments were conducted in triplicate to ensure statistical validity.
- The pH was maintained at 4 using dilute HCl or NaOH.
- The mixtures were shaken at 150rpm and 25°C for 24 hours.
- Solutions were filtered after 24 hours, and metal concentrations were measured using atomic absorption spectroscopy (AAS).

2.6. Statistical evaluation

Statistical analysis was performed using Statistix 8.1 software. The correlation coefficient was calculated to determine the relationship between the biosorption abilities of different (BCs) and the initial HM concentrations. One-way ANOVA was conducted to assess the significant differences between the biosorption capacities of the different algae-derived (BCs). All experiments were carried out in triplicate, and the results were presented as mean \pm standard error.

RESULTS AND DISCUSSION

1. HMs contamination in EH seawater and macroalgae: Impacts on aquatic ecosystems

1.1. HMs contamination in EH seawater

HMs presents a considerable threat to water ecosystems because of their potential to accumulate to toxic levels, thereby causing damage to the ecosystem (Erdoğan & Erbilir, 2007). HMs (Cd, Pb, Ni, Cu, and Zn) were chosen because they are commonly found in industrial effluents and pose significant environmental and health risks due to their toxicity and ability to bioaccumulate in marine organisms. Analysis of seawater samples indicated that the average concentrations of Pb, Cu, Ni, Zn, and Cd were 6.35, 4.09, 1.97, 16.31, 13.06, and 1.97 $\mu\text{g}/\text{L}$, respectively, all exceeding the WHO permissible

limits. However, Mn and Fe concentrations remained within permissible limits (**Zhang et al., 2015**). Mn, being abundant in the Earth's crust with minimal toxicity, plays a significant biological role, especially in aquatic environments (**Zhang et al., 2015**). Although iron oxidation is not toxic in itself, the conversion of its soluble form into insoluble precipitates can block the gills of aquatic organisms (**Okbah et al., 2016**).

The high Cd levels in the EH are associated with sewage discharges from small sewer systems, shipping operations, and sewage disposal in central Alexandria (**Wahbi & El-Greisy, 2016**). Furthermore, the area is subject to effluents contaminated with various human-made materials, including trace metals. Pb, classified as hazardous by the USEPA (2000), originates from manufacturing processes, atmospheric deposition, domestic wastewater, sewage, and sewage sludge (**González-Macías et al., 2014**). Ni discharge into natural waters primarily comes from municipal wastewater, smelting, refining of nonferrous metals, and mine drainage effluents (**Denton et al., 2001; Finkelman, 2005**). Copper concentration in seawater exceeds the World Health Organization (WHO) recommendations by 1.4 times, with permissible limits consistent with those reported by **Wahbi and El-Greisy (2016)**.

Zinc is a prevalent environmental contaminant often found in conjunction with lead and cadmium (**Bhowmik et al., 2010**). Domestic waste discharge represents a significant source of zinc in aquatic environments (**Wafi, 2015**). The findings from the analysis of seven metals (Mn, Cu, Zn, Ni, Pb, Fe, and Cd) in water samples, and three macroalgae species collected from the EH site are summarized in Table (1).

3.1.2. HMs accumulation in macroalgae

Macroalgae have become more popular for their usefulness in monitoring eutrophication, as well as organic and inorganic pollutants. Their capacity to accumulate metals within their tissues has made them valuable biomonitors of metal availability in marine ecosystems (**Gosavi et al., 2004**). The three algae species (*Ulva fasciata*, *Ulva compressa*, and *Corallina officinalis*) collected from the EH area exhibit varying degrees of metal contamination, including Cd, Cu, Fe, Hg, Mn, Ni, Pb, and Zn.

Various types of algae show specific preferences when it comes to accumulating metals. *Corallina officinalis*, a type of red seaweed, showed the highest level of Cd at 19.35µg/ g DW, while the green algae *Ulva compressa* exhibited the highest concentration (12.42µg/ g DW). The increased cadmium concentration in red algae may be due to the higher calcification rate of *Corallina officinalis* in warmer areas, leading to a more relaxed regulation of minor and trace element absorption (**Youssef, 1993**).

The highest concentration of Pb was detected in red algae (*Corallina officinalis*, 40.69µg/ g DW), while the lowest concentrations were observed in green algae, *Ulva fasciata* and *Ulva compressa* (23.33 and 5.0µg/ g DW, respectively). Additionally, *Ulva compressa* exhibited a relatively high Pb concentration (27.51µg/ g DW), possibly due to

its filamentous structure. This observation aligns with the findings of **Benguedda *et al.* (2011)** and **Allam *et al.* (2016)**, regarding the bioaccumulation of Pb and Cd from Béni Saf (Algeria) and Ghazaouet for *Corallina officinalis*, respectively. In addition, *Corallina officinalis* displayed the highest nickel content (35.63 $\mu\text{g}/\text{g}$ DW), potentially because other green algae species (*Ulva compressa* and *Ulva fasciata*) can regulate nickel uptake, leading to lesser accumulation (**Ho, 1987**).

Ulva compressa and *Ulva fasciata* exhibited the highest copper concentrations, followed by *Corallina officinalis* (a Rhodophyta species), consistent with the findings of **El-Din *et al.* (2014)**. *Ulva* species, prevalent along most coastlines, tend to accumulate high nutrient levels in areas affected by domestic sewage, demonstrating a high capacity for binding copper associated with sewage (**Siddiqui & Bielmyer-Fraser, 2019**). Therefore, *Ulva* species could serve as bioindicator species for copper contamination (**Bonanno & Orlando-Bonaca, 2018**).

Manganese levels in *Ulva compressa* ranged from 7.36 to 8.81 g/g DW, with variable trends across sampling sites. Contrary to findings by **Bonanno and Orlando-Bonaca (2018)**, our results indicated higher Mn accumulation in green algae compared to red algae. Iron content exhibited wide fluctuations across different algal species, with *Ulva compressa* > *Ulva fasciata* > *Corallina officinalis*. This variability may be attributed to metal binding to extracellular sites, influenced by chemical and physical conditions of the aquatic environment influencing metal biosorption on algal surfaces (**Mohamed & Khaled, 2005**). The relatively high iron content in three algal species studied is likely attributed to its essential function in biological processes (**El-Sarraf, 1995**).

Ulva compressa showed the highest zinc accumulation (48.13 $\mu\text{g}/\text{g}$ DW), while *Ulva fasciata* and *Corallina officinalis* accumulated zinc at different rates (20.06 and 18.81 $\mu\text{g}/\text{g}$ DW, respectively). This indicates that zinc bioavailability depends on surrounding water concentrations (**El Zokm *et al.*, 2014**), consistent with findings by **Oucif *et al.* (2020)**. Given their metal accumulation capacities, *Corallina* sp. (Cd, Pb, and Ni) and *Ulva* sp. (Fe, Cu, and Mn) could serve as bio-indicator species for metal contamination, complementing the observations made by **Yozukmaz *et al.* (2018)**.

Table 1. Mean and standard errors of HMs concentration in seawater ($\mu\text{g}/\text{L}$) and macroalgae, compared to WHO limits for seawater

	WHO	Seawater	Macroalgae		
			<i>Ulva fasciata</i>	<i>Ulva compressa</i>	<i>Corallina officinalis</i>
Cd	0.11	1.97 \pm 0.53	8.20 \pm 0.25	12.42 \pm 0.87	19.35 \pm 3.42
Pb	0.05	6.35 \pm 0.31	23.33 \pm 1.73	24.58 \pm 0.52	40.69 \pm 1.8
Ni	5.4	16.31 \pm 2.23	25.42 \pm 2.89	22.16 \pm 1.5	35.63 \pm 2.89
Cu	3	4.09 \pm 0.51	17.94 \pm 1.44	18.81 \pm 1.15	15.13 \pm 1.14
Mn	2	1.96 \pm 0.58	6.42 \pm 0.29	7.36 \pm 0.58	3.96 \pm 0.59
Fe	10	5.46 \pm 0.88	287.81 \pm 12.7	437.81 \pm 19	194.06 \pm 6.35
Zn	10	13.06 \pm 1.03	20.06 \pm 1.7	48.13 \pm 4.62	18.81 \pm 2.5

Marine algae demonstrate strong metal biosorption abilities thanks to active functional groups on their cell walls. Using marine macroalgae as activated carbon materials has multiple advantages, including cost-effectiveness, widespread availability, and high efficiency in metal binding (Apiratikul & Pavasant, 2008).

3.2. Bioremediation of HMs using marine BC

Algal BC has been shown to effectively adsorb HMs, including copper (Cu), cadmium (Cd), and zinc (Zn) ions from aqueous solutions (Poo *et al.*, 2018; Son *et al.*, 2018). Biochar derived from the freshwater macroalga *Oedogonium* sp. was used for removing metal ions from industrial effluent produced by a coal-fired power station (Kidgell *et al.*, 2014).

Currently, algae are being employed as precursors for BC production due to their composition of cellulose and hemicelluloses (Jung *et al.*, 2016). The use of marine macroalgae as activated carbon materials presents notable benefits, including low cost, broad availability, and high efficiency in metal binding (Apiratikul & Pavasant, 2008).

3.3. Characterization of macro-algal BC

3.3.1. Energy dispersive x-ray (EDX) analysis

The elemental composition of the three types of biochar (*Ulva fasciata*, *Ulva compressa*, and *Corallina officinalis*) as determined by EDX analysis is shown in Figs. (2, 3, and 4, respectively). Table (2) summarizes the differences between the three types in the percentage of each element, which is presented as a mass percentage and atomic percentage. The results showed that both types of *Ulva fasciata* and *Ulva compressa* have a similar elemental composition that is carbon, oxygen, copper, and cadmium with differences in the percentage of each, while the third type *Corallina officinalis* contains the first three-element (C, O, and Cu) with the absence of Cd. Oxygen is the most abundant in all types with the mass percentage of 56.76, 46.53, and 63.34% for types *Ulva fasciata*, *Ulva compressa*, and *Corallina officinalis*, respectively. The next element in abundance is carbon with a closer mass percentage of 25.44, 23.48 and 27.49% for *Ulva fasciata*, *Ulva compressa*, and *Corallina officinalis*. In types of *Ulva fasciata* and *Ulva compressa*, the cadmium percentage is high compared to that of copper, in *Ulva fasciata* the Cd % is 13.97 compared to 5.80% for Cu, while in the type of *Ulva compressa*, this difference increases between the two elements as the mass percentage of Cd is 23.49% compared to only 2.49% for Cu. On the other hand, cadmium is absent in *Corallina officinalis*, and the mass percentage of Cu increased, compared to the type of *Ulva fasciata* and *Ulva compressa*, to reach 11.21%.

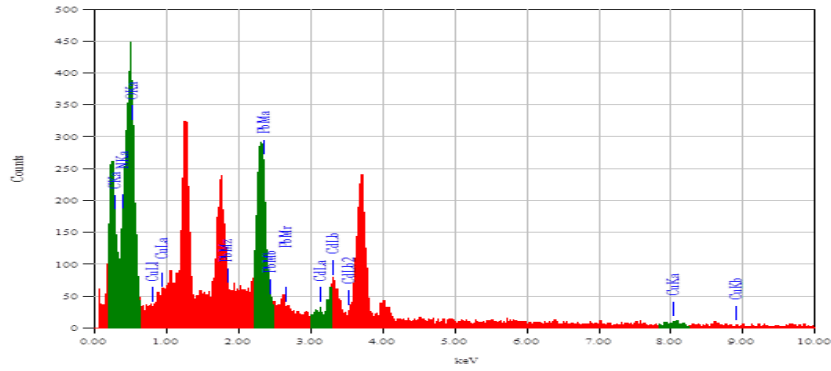


Fig. 2. EDX image of *Ulva fasciata* BC

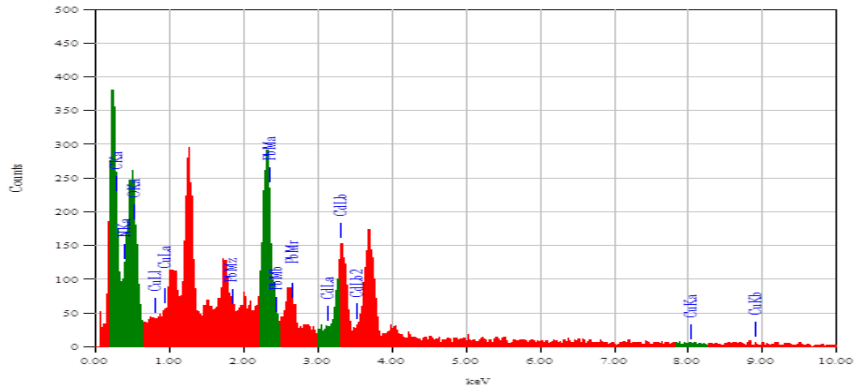


Fig. 3. EDX image of *Ulva compressa* BC

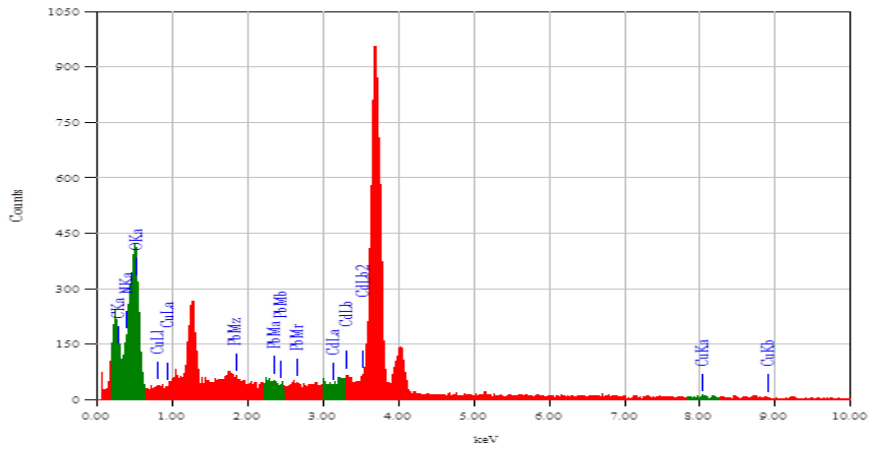


Fig. 4. EDX image of *Corallina officinalis* BC

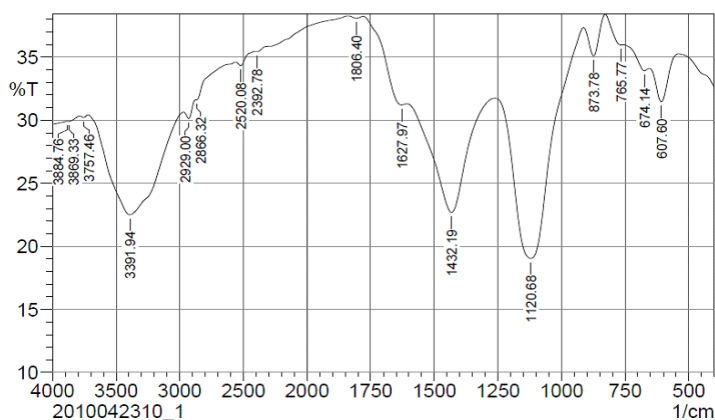
Table 2. The elemental composition of *Ulva fasciata*, *Ulva compressa*, and *Corallina officinalis* BC

Element	<i>Ulva fasciata</i>		<i>Ulva compressa</i>		<i>Corallina officinalis</i>	
	Mass%	Atomic%	Mass%	Atomic%	Mass%	Atomic%
	23.48	34.18	27.49	42.04	25.44	33.87
C	56.76	62.05	46.53	53.41	63.34	63.31
O	5.80	1.60	2.49	0.72	11.21	2.82
Cu	13.97	2.17	23.49	3.84	-----	-----
Cd	100%	100%	100%	100%	100%	100%

3.3.2. Fourier-transform infrared (FTIR) spectroscopy

Research shows that BCs derived from bio-waste are highly effective for extracting toxic metals from wastewater. This effectiveness is attributed to their porous structure, large specific surface area, and rich variety of functional groups (Wang *et al.*, 2019).

The three types of BC underwent analysis to assess various physical properties and chemical structures through several procedures. FTIR spectroscopy was used to identify the functional groups present in the BC samples. FTIR spectra depicted in Figs. (5, 6, and 7) illustrate the absorbance of fundamental functional groups in BC. Additionally, Tables (3, 4, and 5) present the characteristic bands observed in the BC samples, along with their assignments to different functional groups.

**Fig. 5.** FTIR spectra of *Ulva fasciata* BC

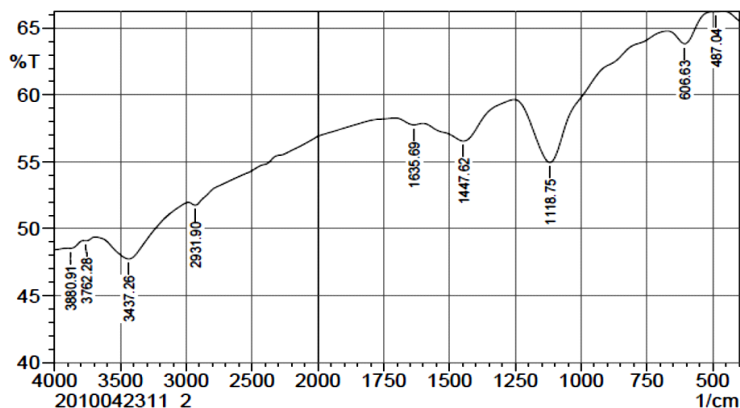


Fig. 6. FTIR spectra of *Ulva compressa* BC

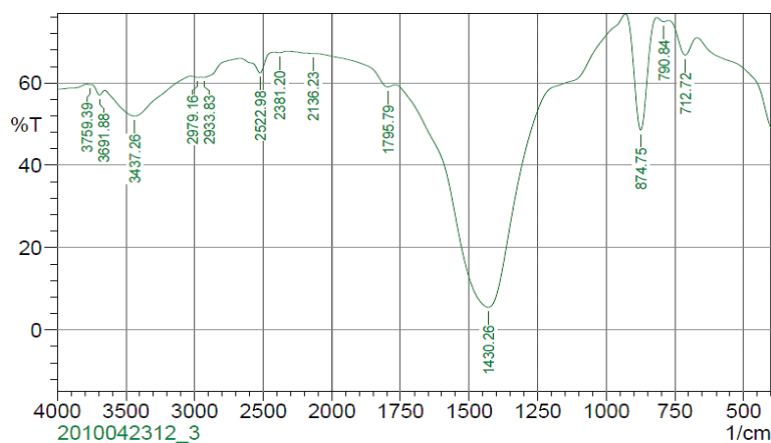


Fig. 7. FTIR spectra of *Corallina officinalis* BC

Table 3. Band assignment to the peaks of BC prepared from *Ulva fasciata*

Stretching frequency	Functional group
3700-3900 (3757.46-3869.33 - 3884.76)	Weak R-OH band representing monomeric alcohol, phenol, carboxylic groups.
3500-3300 (3391.94)	O-H Stretching (intermolecular hydrogen-bonded)
2840-3000 (2929-2866.32)	Stretching C-H group for alkane
2520.08	Stretching -OH group for carboxylic acid
2300-2400 (2392.78)	O=C=O (CO ₂ may be absorbed on the biochar surface)
2000-1650 (1806.4)	Weak bending C-H for aromatic compound
1627.97	C=O
1450-1420 (1432.19)	C-H Asymmetric. Bending
1260-1000 (1120.68)	C-O in carboxylic acids, alcohols, phenols, and esters
880-700 (873.78-765.77)	Bending C-H for 1,3 disubstituted compounds
700-400 (607.60-674.14)	C-C stretching

Table 4. Band assignment to the peaks of BC prepared from *Ulva compressa*

Stretching frequency	Functional group
3700-3900 (3759.39)	Weak R-OH band representing monomeric alcohol, phenol, carboxylic groups.
3700-3584 (3691.88)	Stretching free -OH group for alcohol
3500- 3300(3437.26)	O-H Stretching (intermolecular hydrogen-bonded)
2840-3000(2933.83-2979.16)	Stretching C-H group for alkane
2522.20	Stretching -OH group for carboxylic acid
2300-2400 (2381.20)	O=C=O (CO ₂ may be absorbed on the biochar surface)
2140-2100 (2136.23)	Weak Stretching C≡C for monosubstituted alkyne
2000-1650 (1795.79)	Weak bending C-H for aromatic compound
1450-1420 (1430.26)	C-H Asymmetric. Bending
880±20 (874.75) 780±20 (790.84) 700±20 (712.72)	Bending C-H for 1,3 disubstituted compounds

Table 5. Band assignment to the peaks of BC prepared from *Corallina officinalis*

Stretching frequency	Functional group
3700-3900 (3762.28 -3880.91)	Weak R-OH band representing monomeric alcohol, phenol, carboxylic groups.
3500-3300 (3437.26)	O-H Stretching (intermolecular hydrogen-bonded)
2840-3000 (2931.9)	Stretching C-H group for alkane
1635.69	Carbonyl group C=O
1450-1420 (1447.62)	C-H Asymmetric. Bending
1260-1000 (1118.75)	C-O in carboxylic acids, alcohols, phenols, and esters
700-400 (606.63-483.04)	C-C stretching

3.3.3. Scanning electron microscopy (SEM)

SEM was employed to analyze the microstructure and morphology of the samples after pyrolysis, and this technique is frequently used to study algal BC (De Bhowmick *et al.*, 2018). The SEM images of BC samples prepared from *Ulva fasciata*, *Ulva compressa*, and *Corallina officinalis* are presented in Fig. (8a, b, c, d, e, and f) at different magnifications. The pores and curves on the BC surface appear to be more developed because of the release of low-mass gaseous species during pyrolysis. The surface area of algal BC is rather weakly developed. Increasing temperatures cause the material to agglomerate as a result of the increasing ash content. It is noted that despite the high

magnification, the presence of small-sized granules may explain the high efficiency in the processes of absorption and adsorption.

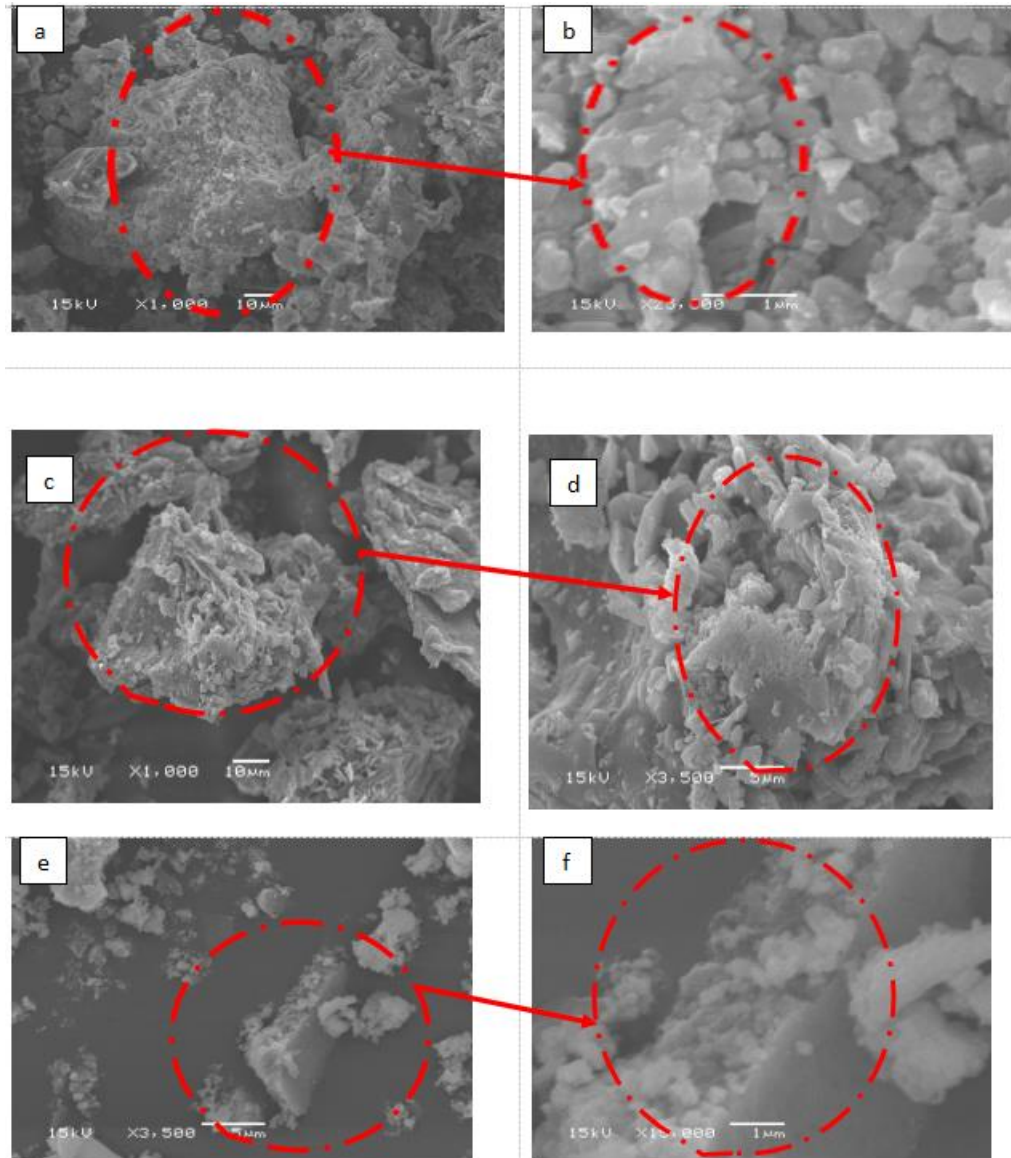


Fig. 8. SEM micrographs of (a, b) for *Ulva fasciata* BC with magnifications of 25000x; (c, d) *Ulva compressa* BC with magnifications of 35000x; (e, f) *Corallina officinalis* BC with magnifications of 15000x

3.3.4. Particle size distribution (PSD)

The PSD of all samples was assessed using the Beckman Coulter N5 Submicron Particle Size Analyzer. The analysis was conducted at two different angles of scatter (90 and 11.1), as shown in Figs. (9, 10, and 11), for samples of *Ulva fasciata*, *Ulva compressa*, and *Corallina officinalis*, respectively. For all samples, the highest intensities of the particles are detected at the larger angle, as shown by the wider distribution curve.

The particle sizes for *Ulva fasciata* and *Ulva compressa* are closer to each other in the large particle size, with a value of 620.9 nm and 666.4nm for *Ulva fasciata* and *Ulva compressa*, respectively. While the particle size of *Corallina officinalis* at the higher angle is larger than that of *Ulva fasciata* and *Ulva compressa*, it is more than twice the size (1541nm). The small particle size, measured at the smaller angle, is less intense, and the size of a small particle in *Ulva compressa* is larger than that in *Ulva fasciata*, and the smallest size for the small particles is recorded for *Corallina officinalis*, as shown for the narrow curve of all samples, with values of 65.1, 98.5, and 39nm for *Ulva fasciata*, *Ulva compressa*, and *Corallina officinalis*, respectively.

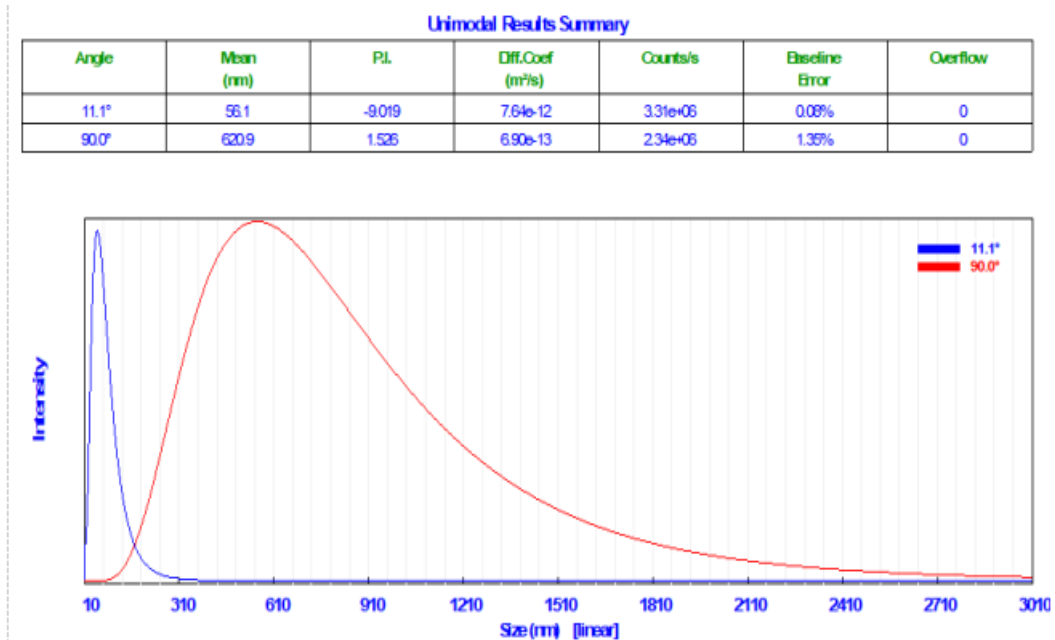


Fig. 9. Particle size analyzing for *Ulva fasciata* BC

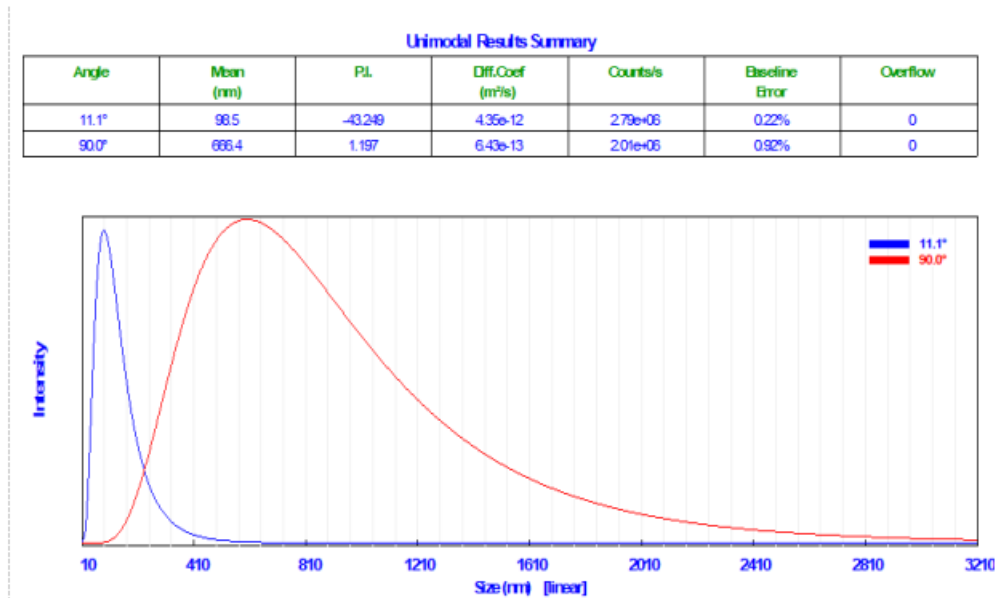


Fig. 10. Particle size analyzing for *Ulva compressa* BC

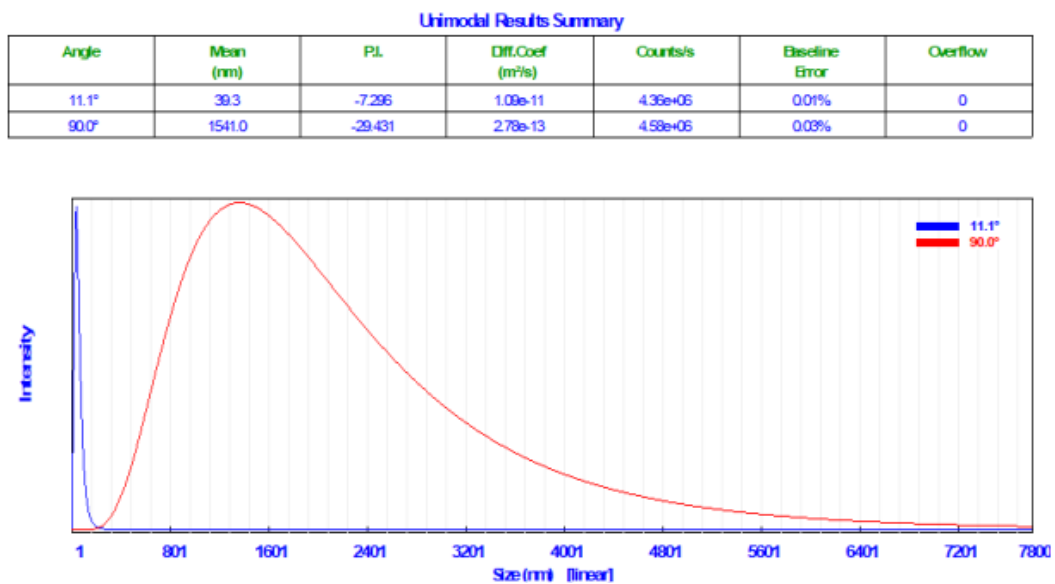


Fig. 12. Particle size analyzing for *Corallina officinalis* BC

3.4. Biosorption research

3.4.1. Impact of initial HM ion concentration

In this study, preliminary experiments were conducted to assess the biosorption of five metals (Cd, Pb, Zn, Ni, and Cu) by BC derived from *Ulva fasciata*, *Ulva compressa*, and *Corallina officinalis* in single-metal solutions. Initially, it was focused on the physicochemical characterization of the BCs, as presented in Table (6).

The subsequent table illustrates the reduction percentages of various HMs following sorption onto the surfaces of the three different algal BC. As indicated in Table

(5), all types of BC exhibited a remarkable effectiveness as sorbent materials for removing high concentrations of HMs from contaminated solutions. Moreover, there were no discernible differences in the efficiency among the three types of BC, with reduction in heavy metal concentration ranging between 97 and 99% for all types, highlighting their exceptionally high biosorption capacities. Our results indicate that the BCs derived from *Ulva fasciata*, *Ulva compressa*, and *Corallina officinalis* have exceptionally high biosorption capacities, with removal efficiencies ranging between 93 and 99% for various HMs. These findings are consistent with previous studies, such as those of **Kidgell et al. (2014)** and **Thivya and Vijayaraghavan (2019)**, who reported high removal efficiencies for BCs derived from freshwater macroalgae and red seaweed, respectively.

Our findings corroborate the substantial biosorption capacity of biochar derived from algal biomass in extracting HMs from contaminated solutions, aligning with previous studies. For instance, **Kidgell et al. (2014)** demonstrated that the BCs produced from the freshwater macroalga *Oedogonium* at 450°C exhibited effective removal efficiencies for Cr (III), Cu (II), and Zn (II) ions from industrial waste, achieving 50% removal for Cr (III), 37% for Cu (II), and 92% for Zn (II). Similarly, **Thivya and Vijayaraghavan (2019)** examined BC derived from red seaweed obtained from *Kappaphycus alvarezii* at 350°C, which displayed efficacy in removing reactive dyes. Additionally, **Gokulan et al. (2019)** highlighted the effectiveness of BC produced from the green seaweed *Ulva lactuca* at 300°C in removing Remazol dyes from complex dye wastewater, achieving a dye removal efficiency exceeding 77.5%. Therefore, the high biosorption capacity of BC samples derived from *Ulva fasciata*, *Ulva compressa*, and *Corallina officinalis* suggests their potential use in treating industrial wastewater and contaminated marine environments. These BC samples could be employed in filtration systems to remove toxic HMs, thereby reducing environmental pollution and protecting aquatic ecosystems.

Furthermore, the results presented in Table (7) demonstrate the superior biosorption of various metal ions by BC materials compared to fresh algae metal accumulation. Specifically, *Corallina officinalis* exhibited maximum absorption of HMs (Cd, Pb, and Ni), whereas *Ulva compressa* demonstrated maximum absorption of HMs (Cu and Zn). Notably, algal BC outperformed fresh algae in removing HMs, indicating its efficacy in environmental remediation. In conclusion, BC derived from *Corallina officinalis* and *Ulva compressa* shows potential as an effective technology for removing metal ions from contaminated environments.

Table 6. Percentage of the biosorption of metals by algal BC

Metal	<i>U. fasciata</i> %	<i>U. compressa</i> %	<i>C. officinalis</i> %
Pb	98.81±0.01	98.93±0.03	98.71±0.03
Zn	99.28±0.11	97.11±0.19	99.58±0.03
Cu	99.86±0.01	99.83±0.02	99.91±0.01
Ni	98.26±0.03	99.43±0.05	97.01±0.07
Cd	99.03±0.03	99.35±0.04	98.99±0.040

Table 7. Comparison of HMs accumulation between fresh algae and algal BC

HMs accumulation (µg/g)		Cd	Pb	Ni	Cu	Zn
<i>U. fasciata</i>	Fresh algae (average)	3.86	24.79	17.12	18.87	21.45
	Algal BC	2417	2967	4350	338	1800
<i>U. compressa</i>	Fresh algae (average)	4.99	21.37	15.29	16.656	33.26
	Algal BC	1.617	2683	1433	422	7217
<i>Officinalis .C</i>	Fresh algae (average)	11.75	40.22	25.08	10.07	18.49
	Algal BC	2517	3217	7467	233	1062

Characterizing BC is crucial to affirm its efficacy in biosorbing the studied HMs. SEM images reveal the presence of small particles, and high magnification supported by particle size distribution studies indicates a high surface area, significantly influencing its biosorption properties (Gai *et al.*, 2014). Additionally, the smooth surface observed in SEM can facilitate the absorption process. FTIR analysis provides a detailed characterization of functional groups present in all types, highlighting the presence of highly oxygenated functional groups. This is further supported by SEM/EDX analysis showing a high percentage of oxygen, indicating potential biosorption sites (Son *et al.*, 2018). Carboxyl and hydroxyl groups on biomass surfaces are recognized for their important role in the biosorption of metals from solutions (Michalak *et al.*, 2018).

CONCLUSION

Our study highlights the pressing issue of heavy metal (HM) contamination in the Eastern Harbor (EH) of Alexandria, where seawater samples showed concentrations of cadmium (Cd), lead (Pb), nickel (Ni), copper (Cu), and zinc (Zn) that exceeded the WHO recommended limits. This severe pollution is primarily driven by sewage effluents, industrial discharge, and municipal wastewater. Among the various macroalgae species tested, *Corallina officinalis* proved to be the most efficient in accumulating cadmium, demonstrating its potential as a key bioindicator and phytoremediator. Other species, such as *Ulva fasciata* and *Ulva compressa*, also exhibited significant heavy metal absorption capabilities, enhancing their potential for monitoring and mitigating HM contamination.

Furthermore, biochar (BC) derived from these algae species demonstrated high removal efficiencies for Pb, Zn, Cu, Ni, and Cd, making it a promising material for environmental remediation. These findings suggest that combining macroalgae with BC can significantly reduce heavy metal pollution in coastal areas. Our research underscores the importance of continuous monitoring of HM contamination in the region and emphasizes the potential of algae-based solutions for environmental cleanup. Future research should focus on optimizing biosorption conditions and exploring the broader application of these techniques in other heavily polluted sites.

REFERENCES

- Abou Gabal, A. A.; Khaled, A. A.; Aboul-Ela, H. M.; Aly, H. M. and Shalaby, O. K. (2021).** Variation of photosynthetic pigments and biochemical screening in some seaweeds from Eastern Harbor, Alexandria, Egypt. *Egyptian Journal of Aquatic Biology and Fisheries*, 25(1), 213-226.
- Abou Gabal, A. A.; Aboul-Ela, H. M.; Khaled, A. A.; Aly, H. M.; Abdullah, M. I. and Shalaby, O. K. (2023).** DNA barcoding of marine macroalgae as bioindicators of heavy metal pollution. *Marine Pollution Bulletin*, 189, 114761.
- Abou Gabal, A. A.; Khaled, A. A.; Aboul-Ela, H. M.; Aly, H. M.; Diab, M. H. and Shalaby, O. K. (2022).** Marine macroalgal biodiversity, spatial study for the Egyptian Mediterranean Sea, Alexandria Coast. *Thalassas: An International Journal of Marine Sciences*, 38(1), 639-646.
- Ahmed Et Al, N. M. (2022).** Accumulation and risk assessment of heavy metals-induced biochemical and histopathological alterations in *O. niloticus* from Lake Nasser, Egypt. *Egyptian Journal of Aquatic Biology and Fisheries*, 26(2), 409-425.
- Alem, A.A. (1993).** The marine algae of Alexandria, Egypt, University Alexandria, 139 p.
- Allam, H.; Aouar, A.; Benguedda, W. and Bettioui, R. (2016).** Use of sediment and algae for biomonitoring the coast of Honaïne (Far West Algerian). *Open Journal of Ecology*, 6(04), 159.
- AOAC, (1990).** "Official methods of analysis 15th Ed", in Association of official analytical chemists, Washington, DC, USA.
- APHA (American Public Health Association) (2017).** Standard Methods for the Examination of Water and Seawater, 23rd Edn. EPA, Washington, USA.
- Apiratikul, R. and Pavasant, P. (2008).** Batch and column studies of biosorption of heavy metals by *Caulerpa lentillifera*. *Bioresour Technol*; 99:2766–77.
- Arif, M.; Liu, G.; Yousaf, B.; Ahmed, R.; Irshad, S.; Ashraf, A. and Rashid, M. S. (2021).** Synthesis, characteristics and mechanistic insight into the clays and clay minerals-biochar surface interactions for contaminants removal-A review. *Journal of Cleaner Production*, 310, 127548.

- Benguedda, W.; Dali Youcef, N. and Amara, R. (2011).** Trace Metals in Sediments, Macroalgae and Benthic Species from the Western Part of Algerian Coasts. *Journal of Environmental Science and Engineering*, 15, 1604-1612.
- Bhowmik, D.; Chiranjib, K.P., and Sampath, K. (2010).** A potential medicinal importance of zinc in human health and chronic disease. *Intern J Pharma Biomed Res.*, 1:0511.
- Bonanno, G. Orlando-Bonaca, M. (2018).** Chemical elements in Mediterranean macroalgae. A review. *Ecotoxicology and Environmental Safety*, 148, 44–71.
- Campanella, L.; Conti, M.E.; Cubadda, F. and Sucapane, C. (2001).** Trace metals in sea grass, algae and mollusks from uncontaminated area in the Mediterranean. *Environmental Pollution*, 111, 117–126.
- Conti, M. E. and Cecchetti, G. (2003).** A biomonitoring study: Trace metals in algae and molluscs from Tyrrhenian coastal areas. *Environmental Reverses*, 93, 99–112. [https://doi.org/10.1016/S0013-9351\(03\)00012-4](https://doi.org/10.1016/S0013-9351(03)00012-4).
- Cui, L.; Noerpel, M. R.; Scheckel, K. G. and Ippolito, J. A. (2019).** Wheat straw biochar reduces environmental cadmium bioavailability. *Environment international*, 126, 69-75.
- De Bhowmick, G.; Sarmah, A.K., and Sen, R. (2018).** Production and characterization of a value-added biochar mix using seaweed, rice husk and pine sawdust: A parametric study. *J. Cleaner Prod.* 200, 641–656.
- Denton, G.R.W.; Bearden, B.G.; Concepcion, L.P.; Siegrist, H.G.; Vann, D.T. and Wood, H.R. (2001).** Contaminant Assessment of Surface Sediments from Tanapag Lagoon, Saipan, Water and Environmental Research Institute of the Western Pacific, Technical Report No. 93, University of Guam, Mangilao, Guam.
- El Zokm, G. M.; Ghani, S. A.; El Naggat, M. F.; Okbah, M. A. and Shakweer, L. (2014).** Comparative study of Zn, Cu, Pb and Cd in water column and suspended matter in the Eastern and Western regions of the Egyptian Mediterranean Sea. In *The 9th International Environmental Conference*, Faculty of Science, Zagazig University, pp. 418-433.
- El-Din, N. S.; Mohamedein, L. I. and El-Moselhy, K. M. (2014).** Seaweeds as bioindicators of heavy metals off a hot spot area on the Egyptian Mediterranean Coast during 2008–2010. *Environmental monitoring and assessment*, 186(9), 5865-5881.
- El-Din, S. N.; Shaltout, N. A.; Nassar, M. Z. and Soliman, A. (2015).** Ecological studies of epiphytic microalgae and epiphytic zooplankton on seaweeds of the Eastern Harbor, Alexandria, Egypt. *American Journal of Environmental Sciences*, 11(6), 450.
- El-Sarraf, W.M. (1995).** Heavy metal content in some marine algae from Alexandria, Egypt. *Bulletin of Faculty of Science of Alexandria University*, 35(2), 475–484.

- Erdoğrul, Ö. and Erbilir, F. (2007).** Heavy metal and trace elements in various fish samples from Sir Dam Lake, Kahramanmaraş, Turkey, *Environmental Monitoring Assessment*, 130: 373-379.
- Finkelman, R.B. (2005).** Sources and Health Effects of Metals and Trace Elements in our Environment: An Overview In: Moore, T.A., Black, A., Centeno, J.A. Harding, J.S. and Trumm, D. A. (Eds.), *Metal Contaminants in New Zealand*, Resolutionz Press, Christchurch, New Zealand, 25-46.
- Fu, F. and Wang, Q., (2011).** Removal of heavy metal ions from wastewaters: a review. *J. Environ. Manage.*, 92, 407–418.
- Gai, S.; Li, C.; Yang, P. and Lin, J. (2014).** Recent progress in rare earth micro/nanocrystals: soft chemical synthesis, luminescent properties, and biomedical applications. *Chemical reviews*, 114(4), 2343-2389.
- Gokulan, R.; Avinash, A.; Prabhu, G. G. and Jegan, J. (2019).** Remediation of remazol dyes by biochar derived from *Caulerpa scalpelliformis*—An eco-friendly approach. *Journal of Environmental Chemical Engineering*, 7(5), 103297.
- González-Hourcade, M.; Dos Reis, G. S.; Grimm, A.; Lima, E. C.; Larsson, S. H. and Gentili, F. G. (2022).** Microalgae biomass as a sustainable precursor to produce nitrogen-doped biochar for efficient removal of emerging pollutants from aqueous media. *Journal of Cleaner Production*, 348, 131280.
- González-Macías, C.; Sánchez-Reyna, G.; Salazar-Coria, L. and Schifter, I. (2014).** Application of the positive matrix factorization approach to identify heavy metal sources in sediments. A case study on the Mexican Pacific Coast. *Environmental Monitoring and Assessment*, 186, 307–324. [Doi:10.1007/s10661-013-3375-0](https://doi.org/10.1007/s10661-013-3375-0).
- Gosavi, K.; Sammut, J.; Gifford, S. and Jankowski, J. (2004).** Macroalgal biomonitors of trace metal contamination in acid sulfate soil aquaculture ponds. *Science of the Total Environment*, 324(1-3), 25-39.
- Ho, Y.B. (1987).** Metals in 19 intertidal macroalgae in Hong Kong waters. *Marine Pollution*, 18, 564–566.
- Ibrahim, N. A.; Abdelghany, E. M.; Shabaka, S.; Ismail, M.; Shalaby, O. and Ismail, M. (2024).** Morphological and molecular characterization of the green algae *Ulva* in the Mediterranean Coast of Egypt. *Regional Studies in Marine Science*, 78, 103807.
- Jung, K.W.; Jeong, T.U.; Kang, H.J. and Ahn, K.H. (2016).** Characteristics of biochar derived from marine macroalgae and fabrication of granular biochar by entrapment in calciumalginate beads for phosphate removal from aqueous solution. *Bioresour. Technol.*, 211, 108–116.
- Kaczala, F.; Marques, M. and Hogland, W. (2009).** Lead and vanadium removal from a real industrial wastewater by gravitational settling/sedimentation and sorption onto *Pinus Sylvestris* sawdust. *Bioresour. Technol.*, 100, 235–243.

- Kenneth, F.; Joniver, C. F.; Meredith, W. and Adams, J. M. (2023).** The productivity effects of macroalgal biochar from *Ulva* Linnaeus bloom species on *Arabidopsis thaliana* Linnaeus seedlings. *European Journal of Phycology*, 58(3), 284-299.
- Khairy, H. M.; Senousy, H. H.; Faragallah, H. M.; Keshta, A. E. and Elshobary, M. E. (2024).** Dynamics of phytoplankton community in the Eastern Harbor and Qaitbay Bay, Alexandria, Egypt: Seasonal abundance and ecological insights. *Egyptian Journal of Aquatic Research*, 50(3), 309-317.
- Khalil, A. N. (1987).** A list of the marine algae from the Alexandria Coast, Egypt. *Bull. Inst. Oceanogr and fish., ARE*, 13(1), 229-241.
- Kidgell, J.T.; De Nys, R.; Hu, Y.; Paul, N.A. and Roberts, D.A. (2014).** Bioremediation of a complex industrial e_uent by biosorbents derived from freshwater macroalgae. *PLoS ONE* 9, e94706.
- Kołodzyńska, D.; Wnętrzak, R.; Leahy, J.J.; Hayes, M.H.B.; Kwapiński, W. and Hubicki, Z., (2012).** Kinetic and adsorptive characterization of biochar in metal ions removal. *Chem. Eng. J.* 197, 295–305.
- Lehmann, J.; Rillig M.; Thies J.; Masiello C.; Hockaday W. and Crowley D. (2011).** Biochar effects on soil biota – A review, *Soil Biology & Biochemistry* 43: 1812-1836.
- Michalak, I.; Mironiuk, M. and Marycz, K. (2018).** A comprehensive analysis of biosorption of metal ions by macroalgae using ICP-OES, SEM-EDX and FTIR techniques. *PLOS ONE*, 13, e0205590.
- Mohamed, L. A. and Khaled, A. (2005).** Comparative study of heavy metal distribution in some coastal seaweeds of Alexandria, Egypt. *Chemistry and Ecology*, 21(3), 181-189.
- Mohan, D.; Sarswat, A.; Ok, Y. S. and Pittman Jr, C. U. (2014).** Organic and inorganic contaminants removal from water with biochar, a renewable, low cost and sustainable adsorbent—a critical review. *Bioresource technology*, 160, 191-202.
- Mohan, D.; Singh, P.; Sarswat, A.; Steele, P.H. and Pittman, C.U. (2015).** Lead sorptive removal using magnetic and nonmagnetic fast pyrolysis energy cane biochars. *J. Colloid Interface Sci.*, 448, 238–250.
- Okbah, M. A.; Masoud, M.; El Zokm, G. M. and Abd El-Salam, A. A. (2016).** Heavy metals distribution in water, particulate and sediment of El-Mex Bay, Alexandria, Egypt. *J. Energ. Environ. Chem. Eng.* 1(1), 1-12.
- Okuku, E. O. and Peter, H. K. (2012).** Choose of heavy metals pollution biomonitors: a critic of the method that uses sediments total metals concentration as the benchmark. *International Journal of Environmental Research*, 6(1), 313-322.
- Oucif, H.; Benaissa, M.; Ali Mehidi, S.; Prego, R.; Aubourg, S. P. and Abi-Ayad, S. M. E. A. (2020).** Chemical Composition and Nutritional Value of Different

- Seaweeds from the West Algerian Coast. *Journal of Aquatic Food Product Technology*, 29(1), 90-104.
- Poo, K.M.; Son, E.B.; Chan, J.S.; Ren, X.H.; Choi, Y.J. and Chae, K.J. (2018).** Biochars derived from wasted marine macro-algae (*Saccharina japonica* and *Sargassum fusiforme*) and their potential for heavy metal removal in aqueous solution. *J. Environ. Manag.* 206, 364–372.
- Premarathna, K. S. D.; Rajapaksha, A. U.; Sarkar, B.; Kwon, E. E.; Bhatnagar, A., Ok, Y. S. and Vithanage, M. (2019).** Biochar-based engineered composites for sorptive decontamination of water: A review. *Chemical Engineering Journal*, 372, 536-550.
- Rasheed, M.; Saeed, I. and Ibrahim, O. (2024).** Study of Pollution by Some Heavy Metals in the Water of the Tigris River in Some Areas of Salah Al-Din Governorate. *Egy J Aqua Biol & Fish.* 28(2): 317 – 326.
- Salaah, S. M.; Zanaty, N. and El-Naggar, M. M. (2022).** Evaluation of heavy metals contents and the possible risk in the surface water and fish of Lake Qarun, Egypt. *Egyptian Journal of Aquatic Biology and Fisheries*, 26(4), 1067-1091.
- Salgado, L. T.; Andrade, L. R. and Filho, G. M. A. (2005).** Localization of specific monosaccharides in cells of the brown alga *Padina gymnospora* and the relation to heavy-metal accumulation. *Protoplasma*, 225, 123-128.
- Siddiqui, S. and Bielmyer-Fraser, G. K. (2019).** Accumulation and Effects of Dissolved and Nanoparticle Silver and Copper in Two Marine Seaweed Species. *Georgia Journal of Science*, 77(2), 1.
- Son, E.B.; Poo, K.M.; Chang, J.S. and Chae, K.J. (2018).** Heavy metal removal from aqueous solutions using engineered magnetic biochars derived from waste marine macro-algal biomass. *Sci. Total Environ.* 615, 161–168.
- United State Environmental Protection Agency (2000).** Risk- based concentration table, Philadelphia PA, Washington DC United States.
- Vargas E Silva, F. and Monteggia, L. O. (2015).** Pyrolysis of algal biomass obtained from high-rate algae ponds applied to wastewater treatment. *Frontiers in Energy Research*, 3, 31.
- Wafi, H. N. (2015).** Assessment of heavy metals contamination in the Mediterranean Sea along Gaza Coast-A case study of Gaza fishing harbor. Master Thesis, Al-Azhar University-Gaza.
- Wahbi, O. M., and El-Greisy, Z. A. (2016).** Impact of water quality at different locations of Alexandria mediterranean coast on the pituitary-ovarian axis of gilthead seabream *sparusaurata*. *Journal of Fisheries and Aquatic Science*, 11, 244-254.
- Wang, H.; Zhang, M. and Lv, Q. (2019).** Removal efficiency and mechanism of Cr (VI) from aqueous solution by maize straw biochars derived at different pyrolysis temperatures. *Water*, 11, 781.

- Youssef, D.H. (1993).** Studies on some inorganic chemical constituents of marine algae in relation to their environments. Master Thesis. Faculty of Science, Mansoura University, Egypt.
- Yozukmaz, A.; Yabanli, M. and Sel, F. (2018).** Heavy metal bioaccumulation in *Enteromorpha intestinalis*, (L.) Nees, a macrophytic algae: the example of Kadin Creek (Western Anatolia). *Brazilian Archives of Biology and Technology*, 61.
- Yuan, P.; Wang, J.; Pan, Y.; Shen, B. and Wu, C. (2019).** Review of biochar for the management of contaminated soil: Preparation, application and prospect. *Science of the total environment*, 659, 473-490.
- Zhang, S.; Tao, L.; Jiang, M.; Gou, G. and Zhou, Z. (2015).** Single-step synthesis of magnetic activated carbon from peanut shell. *Mater. Lett.*, 157, 281–284.
- Zhang, W.; Mao, S.; Chen, H.; Huang, L. and Qiu, R. (2013).** Pb (II) and Cr(VI) sorption by biochars pyrolyzed from the municipal wastewater sludge under different heating conditions. *Bioresour. Technol.*, 147, 545–552.
- Zhao, C.; Wang, B.; Theng, B. K.; Wu, P.; Liu, F.; Wang, S. and Zhang, X. (2021).** Formation and mechanisms of nano-metal oxide-biochar composites for pollutants removal: A review. *Science of the Total Environment*, 767, 145305.